DOI: 10.1590/2317-4889201820170090

ARTICLE

Low-temperature metamorphism in the Capiru Formation, Morro Grande Synform, Southern Ribeira Belt

Larissa da Rocha Santos[1]*, Renato Leandro[2], Anelize Bahniuk[3], Leonardo Fadel Cury[4]

ABSTRACT: *The Capiru Formation consists of a low-grade meta-sedimentary succession of slates, phyllites, quartzites and marbles, disposed in blocks delimited by thrust and strike-slip faults in the Curitiba Terrane, Southern Ribeira Belt, Southern Brazil. The metamorphic and deformation records are heterogeneous, with deformed zones tectonically interbedded by domains with preserved sedimentary features. The present work aims to understand the development of mineral paragenesis based on geochemical and petrographic analysis. We selected samples of metasandstones, slates, phyllites and rhythmic phyllites, with different metamorphic and deformation records to be analysed. We selected samples with different metamorphic records to be analysed. The petrographic characterization of foliations was made through field studies supported by microtectonic analysis. The mineralogical and chemical compositions were determined by X-ray diffractometry and X-ray fluorescence, respectively. The results show a preserved sedimentary bedding (S_0), defined by sedimentary structures with top-and-bottom indicators. The S_1 foliation is related to a thrust tectonics, and it is characterized by a continuous slaty cleavage. The S_1 slaty cleavage is crenulated and cut by a millimetric S_2 cleavage. The mineral assemblage is composed by quartz, sericite, magnetite/goethite and carbonaceous material. The metamorphism was developed under low-temperature conditions (between 250–350°C) and low pressure gradients (2.5–4.5 kbar). The geotectonic environment is considered as a thrust-and-fold-belt system, with structures developed in superior crust levels.*

KEYWORDS: *Capiru Formation; low-grade metamorphism; Southern Ribeira Belt; tectonic evolution.*

INTRODUCTION

Integrated studies of metamorphic petrology and structural geology are important tools to understand the tectonic evolution in orogenic interior zones. However, relationships between metamorphic mineral growth, different deformation phases and the control of developed tectonic structures is challenging in low-grade terrains (Poyatos *et al.* 2001).

Rocks formed in low-grade metamorphic conditions are commonly identified by the abundance of hydrated minerals, fine grains, disordered crystallized structures, with considerable compositional variation that represents chemically and structurally metastable phases in the phyllosilicates (Sassi & Scolari 1974).

In terms of low-temperature metamorphism, the recrystallization is often not immediately obvious due to the fine-grained scale of the products. Also, the apparent lack of regularity in the metamorphic development and the partial recrystallization with many relict features of the protolith point to non-equilibrated systems without obvious overall controls (Robinson & Merriman 1999). Given these facts, the key to study low-grade terrains take into consideration metamorphic reaction progress and the original minerals transformation within their respective polytypes.

Metamorphic petrology techniques by optical microscopy combined with geochemical analysis that quantifies the progression of metamorphic reactions could provide information on orogenic complexes and their different portions in a structural context. Correlations between deformation, reaction progress and metamorphic grade in deformed areas under low- and very low-grade metamorphism have been examined by some authors. Roberts and Merriman (1985)

[1]Programa de Pós-graduação em Geologia Exploratória, Departamento de Geologia, Laboratório de Minerais e Rochas – Universidade Federal do Paraná – Curitiba (PR), Brasil. *E-mail: lrsantos.geo@gmail.com*

[2]Programa de Pós-graduação em Geologia Exploratória, Departamento de Geologia, Universidade Federal do Paraná – Curitiba (PR), Brasil. *E-mail: renatole@hotmail.com*

[3]Departamento de Geologia, Laboratório de Minerais e Rochas – Universidade Federal do Paraná – Curitiba (PR), Brasil. *E-mail: anelize.bahniuk@ufpr.br*

[4]Departamento de Geologia, Laboratório de Minerais e Rochas – Universidade Federal do Paraná – Curitiba (PR), Brasil. *E-mail: cury@ufpr.br*

*Corresponding author.

Manuscript ID: 20170090. **Received on:** 07/08/2017. **Approved on:** 01/07/2018.

interpreted a causative relationship between strain and low metamorphic grade from the association with an anticline geometry. Gutiérrez-Alonso and Nieto (1996) established a semi-quantitative relationship between illite cristallinity and finite strain, related to the distance from an important thrust across a large Variscan structure.

Poyatos *et al*. (2001) obtained X-ray diffraction data suggesting that the rocks did not reach the equilibrium, but strain effects favored the progress of mineral reaction in deformed sectors, from syn-kinematic studies of the very low-grade metamorphism in a polyphase deformed Variscan sector.

Potel *et al*. (2006) investigate the very low-grade metapelites of the Koumac and Diahot terrains in New Caledonia, using the illite cristallinity and b_o cell dimensions of K-white micas, and demonstrate that the b_o cell dimension provides a robust estimate of maximum pressure reached in low-temperature domains with polyphasic metamorphic histories.

The aim of this study is to estimate the local conditions of low-grade metamorphism in a polyphasic deformed area in the Capiru Formation, at Morro Grande region, emphasizing the analytical techniques applied with the purpose of understanding the early stages of metamorphic development, related to the tectonic and structural contexts in which these rocks were formed.

Quantitative studies of progressive metamorphic reactions in low-grade rocks should take into account a number of variables influencing the results: compositional variations of protoliths, chemical availability, amount of circulating fluids, porosity and permeability; their association with tectonic structures should be well established, in order to understand the main mechanisms that affect the reaction progress (Frey 1991). Due to the complexities of understanding the combination of main controls, studies for this purpose should be extremely detailed.

For this study, two detailed cross-sections were chosen aiming to understand the early stages of metamorphic development. Differences in deformation intensity or deformation phases developed in a progressive system can be recognized in the cross-sections, providing a wide range of contingencies to test correlations between crystal-chemical data, organic matter maturation index and petrographic features under local conditions.

The selected sites for the detailed study were the preserved stratigraphic succession sectors within a well-known structure in Capiru Formation, the Morro Grande Synform (MGS). The MGS, extensively studied by Fiori (1991, 1994), Fiori and Gaspar (1993) and Leandro (2016), consists of two large thrust units, composed of a stack of several slices showing variable strain, with preserved inner sectors and intensely deformed edges. Lithologies include laterally homogeneous siliciclastic rocks, suitable for low-grade parameters determinations.

GEOLOGICAL SETTING

The Capiru Formation, defined by Bigarella and Salamuni (1956), is a supracrustal unit of the Curitiba Terrain (Siga Jr. 1995). It is characterized by lithologic units composed of meta psammites, metapelites, and metadolomites product of low-grade metamorphism, disposed in blocks delimited by significant thrust faults (Fiori 1991, 1994, Fiori & Gaspar 1993).

The rocks of the Capiru Formation crop out as folded and elongated zones, mostly in NE-SW trending, bounded on the north by the Lancinha Shear Zone (LSZ), and to the south by the Atuba Complex rocks (Fig. 1).

There are at least two tectonic-metamorphic events in the Capiru Formation (Fiori 1991). One was related to a thrust tectonics and another related to a transpressive tectonics with strike-slip shear zones and their related structures (Fiori 1991).

The thrust tectonic event was responsible for the development of a regional phase of progressive metamorphism under greenschist facies conditions (biotite zone), whereas the transpressive event deformed the previous records in a large scale fold system, which generate paregenesis restricted to the mylonite zones (Leandro 2016).

The metasedimentary rocks of the Capiru Formation display intensely deformed tectonofacies contrasting with preserved stratigraphic successions, containing relict sedimentary structures, such as those described by Bigarella and Salamuni (1956), Fiori and Gaspar (1993), Juschaks (2006), Bahniuk (2007), Silva (2010), Leandro (2016), and Leandro *et al*. (2017).

Based on geochronological studies, Leandro (2016) considers the Capiru Formation as an allochthonous unit in a thrust-and-fold belt context. U-Pb ages obtained in detrital zircons from the Morro Grande unit show strong peaks at 2.1 Ga. However, the weighted mean age of the youngest concordant zircons yield maximum deposition ages of 1.08 Ga.

Morro Grande Synform (MGS) structure

The MGS rocks crop out on the north side of the city of Colombo, southern Brazil (Fig. 1). The synform presents a W-E trend, with 70 km^2 of exposure. The axial plane shows approximate N70 strike and moderate dip angles around 60º towards SE, comprising a regional synform with an inverted flank (Fiori 1991).

The Capiru Formation is subdivided, bottom-to-top, in three lithological sets: Juruqui, Rio Branco and Morro Grande, delimited by thrust faults. The stratigraphic sequence of Capiru Formation and paleoenvironmental interpretations are described in detail by Fiori and Gaspar (1993), suggesting a marine environment to the sedimentation of the lithological sets.

Juschaks (2006), Bahniuk (2007) and Silva (2010) interpreted a tide participation in a shallow marine environment in the metadolomites from Rio Branco set.

Leandro (2016) implies an estuarine environment with sporadic subaerial exposition to the Morro Grande set. The literature about structural geology, regional relevance and tectonic evolution models are described by Fiori (1991), Fiori (1994), Fiori and Gaspar (1993), and Leandro (2016).

The Capiru Formation in the Morro Grande region includes, from bottom to top:

- A ferruginous sequence with quartzites, metasandstones and metaconglomerates with goethite cement and phyllites with magnetite;
- A sequence of metasiltites, meta-argilites, metarhythmites and metasandstones with carbonaceous material.

Both sequences from the Morro Grande set are tectonically settled above dolomitic carbonates, interbedded with phyllites and quartzite lenses, from Rio Branco set.

METHODS

Firstly, a detailed analysis of the previous works in Morro Grande Synform was carried out, focused mainly on the identification of possible sectors with preserved sedimentary structures, stratigraphic succession and representative lithotypes. From the previous geological surveys, two sites showing original stratigraphy were chosen to obtain two detailed 1:500 cross-sections.

Sampling

Twenty-four samples from the corss-sections were collected for the petrologic study of metapelites and metasandstones of the Capiru Formation in Morro Grande region. The sampling focused on homogenous and representative lithotypes, distant from fractured zones, also avoiding weathered rocks. Samples were all collected, while measuring stratigraphic sections, in areas of lower deformation. After sampling procedures, the following analytical techniques were

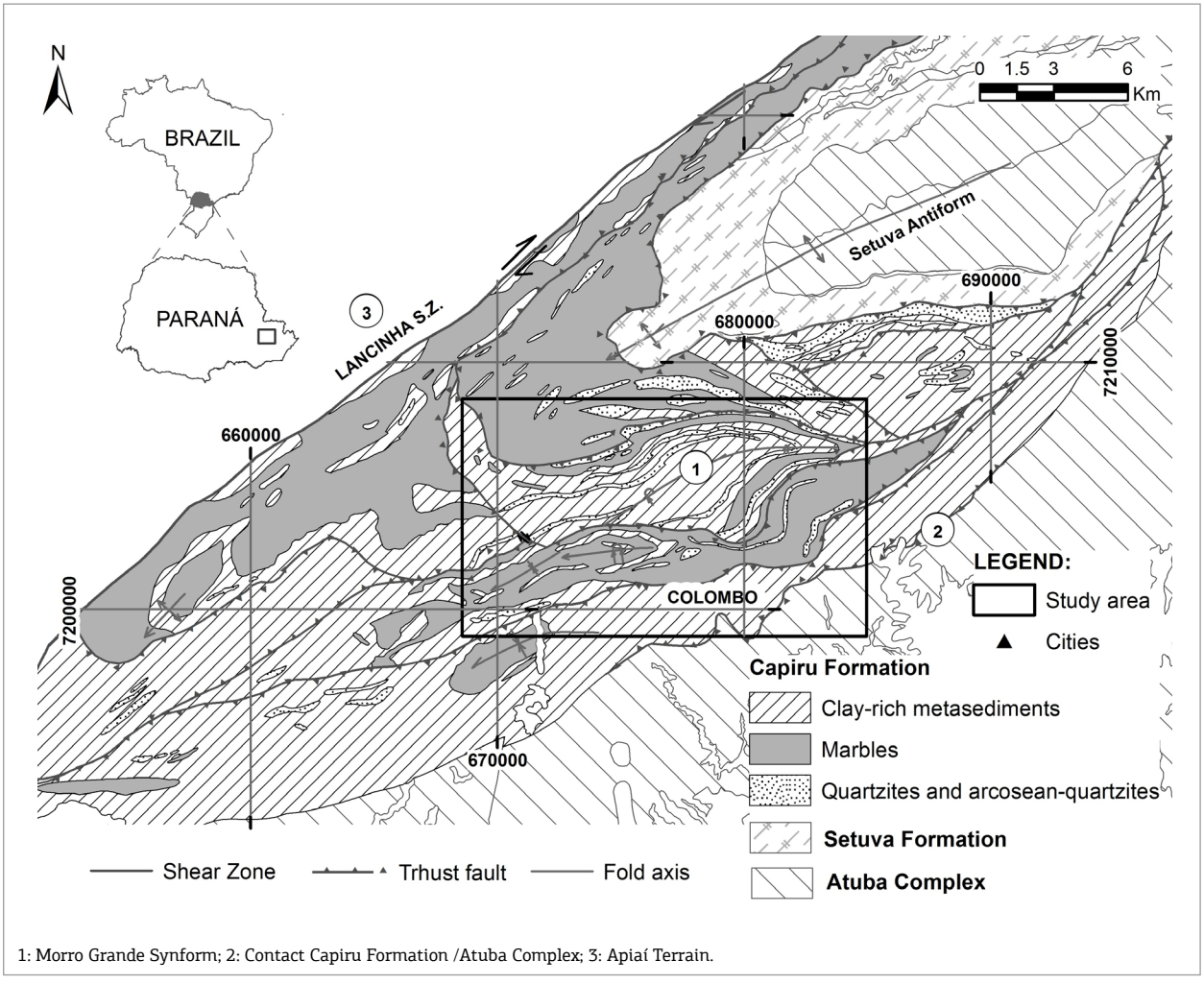

1: Morro Grande Synform; 2: Contact Capiru Formation /Atuba Complex; 3: Apiaí Terrain.

Figure 1. Simplified geologic map of the Capiru Formation and location of study area. Adapted from Fiori (1985).

performed at Mineral and Rock Analysis Laboratory, Federal University of Paraná, Brazil (LAMIR-UFPR):

Scanning Electron Microscopy (SEM)

Samples of the main lithotypes including metapelites and metasandstones were analyzed by scanning electron microscopy – secondary electrons (SEM-SE) to identify and quantify the mineral phases used in the crystal-chemical parameters study. In addition, SEM was used to recognize possible secondary clay-minerals product of weathering.

SEM – energy dispersive spectroscopy (SEM-EDS) analyses were performed in rock matrix disaggregated grains to evaluate the chemical characterization of mica aggregates, framework grains and accessory minerals.

SEM analyses were performed in rock tablets, with a JEOL 6010LA instrument and the surfaces were gold coated.

After initial treatment by washing for elimination of superficial oxides and scanning electron microscopy analyses, the lithotypes were powdered in mortar until a homogenous powder was obtained, to perform the following analytical techniques:

Chemical analysis by X-ray fluorescence (XRF)

Powdered samples from the main lithotypes were analysed by X-ray fluorescence using the quantitative method in a specific line for silicate rocks, sand, clays and talc, to quantify the major oxides (SiO_2, Al_2O_3, Fe_2O_3, CaO, MgO, K_2O, Na_2O, TiO_2, MnO and P_2O_5). Fused beads containing 9 g of lithium tetraborate were made using a 0.9 g sample aliquote. The loss on ignition (LOI) was determined from 0.5 g of dry sample and heated afterwards to 1,000ºC for a two-hour period. Bulk rock analyses were made by XRF on a spectrophotometer Panalytical AXIOS MAX.

X-ray diffractometry (XRD)

Aliquots of bulk rock powder were separated and analyzed. The < 2 μm fraction was obtained from the dispersion of 10 g of pulverized sample diluted in 100 mL of distilled water.

After the decantation period, the < 2 μm fraction was drained and exposed on glass slides oriented aggregates. XRD analyses were made in a diffractometer Panalytical Empyrean equipped with a graphite monochromator, using CuKα radiation, 40 kv,30 mA generator settings and fixed 1º divergence slit. The analyzed range was from 2θ 2 to 30º. Peaks widths were calculated from reflections on Δº2θ, using the X'Pert HighScore software and the minerals were identified by comparison with the 2002-PDF2-ICDD database.

Muscovite/illite 'crystallinity' index ('C'I)

The 'C'I was measured from the air dried, ethyleneglycol treated and heated sample diffractograms, obtained through ~10 Å reflection of white mica (K-mica). The 'C'I was measured by the width of the peak at half-height (FWHM) of the first basal reflection of illite on XRD patterns. Using the indexes standardized by Kübler (1968), the typical limits of the anchizone are 0.25–0.42Δº2θ, and are subdivided in low ('C'I > 0.30 Δº2θ) and high ('C'I < 0.30 Δº2θ) anchizone (Merriman & Peacor 1999). The epizone is represented by values lower than 0.25 Δº2θ, and can be correlated with the low metamorphic grade (Frey 1987).

The 'C'I represents an indicator of reaction progress and the obtained temperatures must be considered as approximate, and cannot be admitted as an actual geothermometer (Merriman & Peacor 1999). The numerical value of the 'C'I diminishes at greater crystallinity and higher temperature. Although temperature is claimed to be the main factor controlling illite crystallinity, it is by no means the only one. It also depends on factors such as the composition of the sediment and the fluid phase, the porosity and permeability, the admixing of detrital mica and authigenic illite, the illite crystal chemistry, tectonics and the laboratory conditions under which it is measured (Frey 1991). For the purpose of this work, however, the differences between the values are much more important than their absolute values.

The FWHM values were measured using the X'Pert HighScore software and the results expressed in terms of the Bragg angle 2θ.

Basal spacing of K-mica (d-spacing)

Measurements of basal space (d-spacing) of K-mica were done using the < 2 μm fraction samples. The phyllosilicate basal spacing is related with its compositional characteristics (Guidotti *et al.* 1992), and can represent the paragonite content (K for Na substitution) at the inter-lamellar sites, reflecting, approximately, its formation or reequilibrium temperature.

However, other factors might reflect on this parameter, like the phengite content (Guidotti 1984, Guidotti *et al.* 1992), and the presence of minor quantities of NH_{4+}, F^- or OH for O^- substitution (Juster *et al.* 1987, Robert *et al.* 1993, Ackermann *et al.* 1993).

White mica b_0 cell dimension

Pelitic rock compositions containing predominantly the 'quartz-muscovite' assemblage were used to measure the K-mica b_o cell dimension. The dimensions were determined in samples free of paragonite and interstratified clay-minerals. Rocks with elevated quartz content were avoided through b_o cells analyses, following the procedures suggested by Guidotti and Sassi (1986).

The analyses were performed along rock slices cut perpendicularly to the slate cleavage and in the powder whole-rock sample fraction. The range 58–63º2θ was scanned at 0.5º 2 θ/min and b_o cell determined from the peak reflection (060) of white mica.

The average value of b_o cell was calculated from six determinations of each sample. After comparison between values obtained from the polished slices and the powder whole-rock aliquot, a standard deviation of σ = 0.0003 was noted, considered to be insignificant for the sample population. After the preliminary analyses, we chose to use the powder disoriented samples to perform the b_o cell study.

The b_o cell dimension of white mica depends exclusively on the phengite substitution, which is related with pressure conditions at the crystallization/recrystallization time. For this reason, a semi quantitative relationship is established between the b_o cell dimension and the metamorphic pressure gradient. Values lower than 9.000 Å are typical of low-pressure metamorphism, whereas values higher than 9.040 Å are typical of high-pressure facies (Guidotti & Sassi 1986).

Bulk organic carbon content (BOC)

The bulk organic carbon content (BOC) of meta-argilites and carbonaceous phyllites was obtained by the dry combustion method, using an infrared C, H and N analyzer, LECO Truspec CHN at the Soils Laboratory - UFPR. The procedure used a 0.25 g powdered sample aliquot. There was no need to follow the step of inorganic carbon removal, since XRD and XRF did not show inorganic carbon content.

Pre-Cambrian rocks kerogens have seen metamorphic grades to at least very low-grade metamorphism. Most kerogens are notoriously difficult to characterize because of the heterogeneous nature of the components and their polymeric nature. A primary measure of composition comprises the elemental abundances, especially in respect to C, H, O, N, and S. Thermal maturation leads to progressive loss of H, N, O, and S relative to carbon, which is the end-stage product in metamorphosed sediments (Summons & Hallmann 2014).

Heat-driven release of hydrocarbons, nitrogen, and CO_2 leads to residual kerogens with progressively lower H/C and N/C values (Summons & Hallmann 2014, Watanabe *et al.* 1997). Due to this, the quantities of these elements were obtained in order to represent a qualitative relation of the thermal maturation in the organic matter and to compare the results obtained through the white-mica crystal-chemical parameters.

RESULTS

The metapelites and meta psammites samples were studied aiming to describe the mineralogical assemblages. The studied lithotypes comprise metasedimentary rocks with main planar surface given by the primary sedimentary bedding (S_0), evidenced by the presence of different compositional and textural characteristics, planar lamination (Fig. 2A) and other preserved sedimentary structures, such as inverse graded bedding, cross stratification, climbing ripples, hummocky cross stratification and linsen and flaser structures.

The lithotype classification was performed with the following criteria:

- Recognition of the protolith;
- Structural classification, when the protolith features were not recognized.

The cross-sections in Figure 3 display, from bottom to top, metric layers of granoblastic quartzite in contact with meta-carbonatic rocks. The quartzites are medium to coarse grained, homogenous, white to yellow, with microstructures such as undulatory extinction and sutured contacts (Fig. 2B).

The metasandstones occur as metric lenses and layers, being fine to coarse grained with rounded quartz (Fig. 2C) and feldspar framework, with fine grained sericite matrix, which may contain magnetite. Goethite occurs as cement, giving a reddish aspect to the rocks (Fig. 2D). Sepiolite may occur in the matrix in the contact with the carbonate rocks. Kaolinite is restricted to the micro pores.

Detrital muscovite grains are observed in some metasandstones, showing deformation features between quartz framework grains and rough and ragged boarders.

Metasiltites are finely laminated, composed by quartz and sericite, with magnetite in the matrix. Metasiltites occur interbedded with gray meta-argillites associated with carbonaceous material. The rhythmic silt/clay interbedding represents the dominant lithotype in the Morro Grande region (Fig. 2A).

Metric lenses of metaconglomerates occur subordinately, with millimiter-sized rounded quartz framework, and quartz-sericite matrix. Cements of goethite and kaolinite are common.

The tectonofacies observed are carbonaceous phyllites composed by sericite, and organic matter and ferruginous phyllites with sericite-quartz-goethite or magnetite assemblage.

The metapelites and meta psammites are composed of quartz and sericite, representing 60 to 90% of the total of rocks. Kaolinite and iron oxides may represent 5 to 10% of the bulk rock composition. The common accessory minerals are rutile, ilmenite, zircon, titanite and monazite.

Goethite massive layers occur in the ferruginous sequence, showing centimetric thickness (0.5–2 cm) parallel to the sedimentary bedding (S_0) and interbedded with metasandstone layers.

The metapelites present a lamination defined by alternating quartz-rich and sericite-rich beds, with variable thickness (Fig. 2A).

Preferred oriented sericite occurs on layers where phyllosilicates predominate, characterizing a slaty cleavage, subparallel to the primary lamination (S_0), with regular development (Fig. 2A).

The foliation in metasandstone beds is defined by the orientation of elongated quartz and sericite (when existent in the matrix) in regular domains (Fig. 2B).

The slaty cleavage in the metapelites and metasandstones in Capiru Formation is classified as S_1, developed in a structural context where it is still possible to recognize original structures and relict grains with sedimentary aspects (Fig. 4A). There is an angle variation on S_1 cleavage in the quartz-rich beds within the metapelites, product of refraction, suggesting a superior structure level development.

The S_1 cleavage presents direction close to the S_0 sedimentary bedding, and dips with differences between 15–30º, suggesting a tight to isoclinal folding, where pressure solution is a dominant process (Figs. 4B and 4C).

Locally, the minerals oriented on S_1 slaty cleavage are perturbed by a subparallel surface, portraying slight variable spacement (millimetric to centimetric) with absence of mineral growth. This surface was heterogeneously developed, characterizing the beginning of a crenulation cleavage S_2, which might dissolve rupture or fold S_1 planes (Fig. 4D).

Structural context

At least two tectonic events are recognized in the Capiru Formation, a thrust-tectonic system, after deformed by a

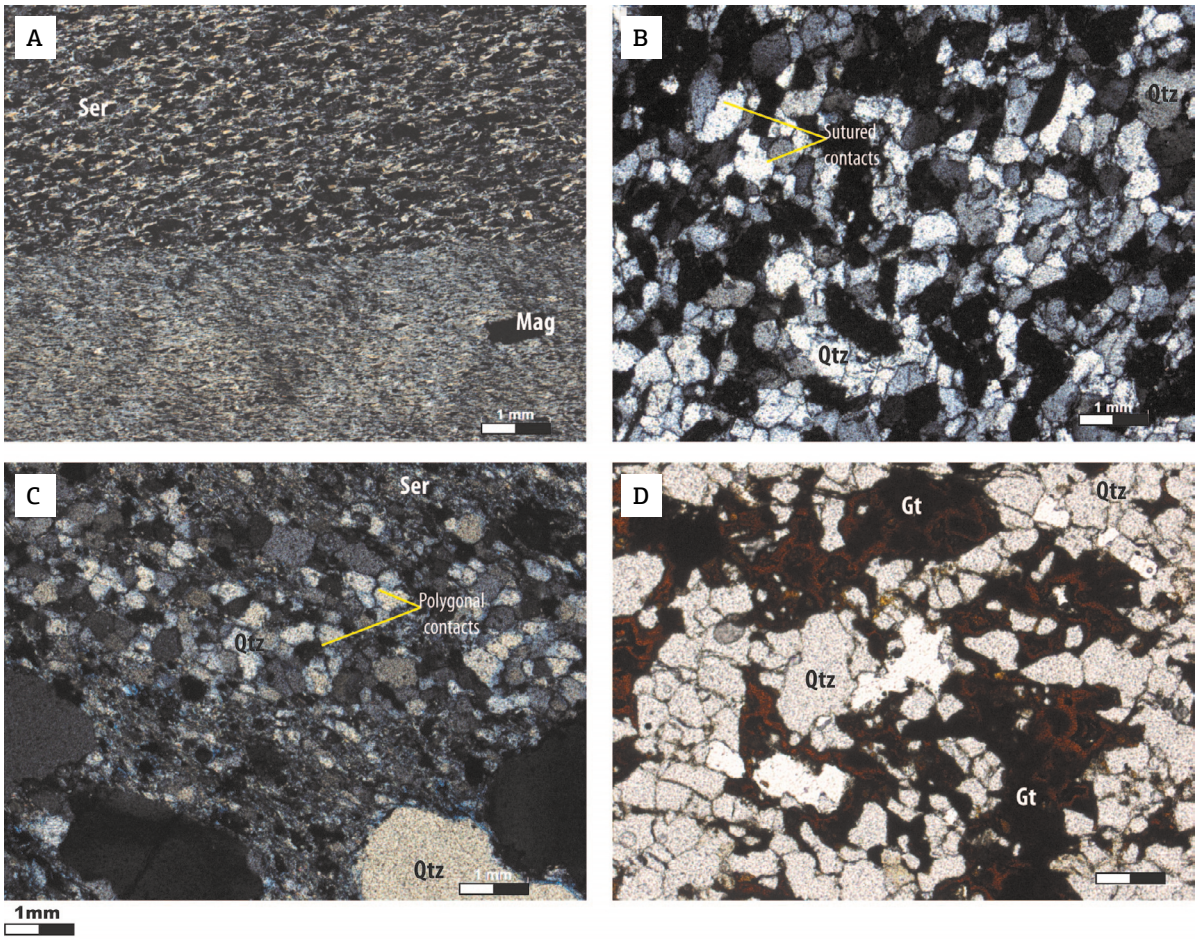

Figure 2. Photomicrographies of the Capiru Formation in the Morro Grande region. (A) Metarhythmite – or slate – showing preserved S_0 sedimentary bedding, cross-polarized light (cpl). Sample MG-03. (B) Homogeneous granoblastic quartzites showing intracrystalline deformation of the quartz grains, in a strong undulatory extinction. Notice sutured contacts (cpl). Sample MG-35. (C) Meta-arenites with qtz-ser matrix. The meta-arenites framework shows sedimentary aspect with preservation of clay-coating. The matrix quartz grains present undulatory extinction and polygonal contacts (cpl). Sample MG-15. (D) Quartzites with ferruginous cement composed of goethite. Uncrossed polarizers (ucp). Sample MG-25. Abbreviations used for minerals are those suggested by Kretz (1983).

transpressive event (Fiori 1991, 1994, Fiori & Gaspar 1993, Siga Jr. 1995, Faleiros *et al.* 2011).

The most remarkable structural feature of the Capiru Formation lithotypes are the differences within the structures development, but in diachronic genesis within the same tectonic context.

The thrust-tectonic in the Morro Grande region is characterized by the heterogeneous development of foliations, which can be related to the intensity of cleavage varying from its incipient form to a fully developed S_1 slaty cleavage towards the faults. These faults are characterized as low-angle shear zones that generate tectonofacies recognized in field as phyllites and quartzites in diachronic development with S_1 foliation.

The Tranqueira-Pessegueiro and Morro Grande faults (Fig. 3) show N45-70E direction, with movement toward SE to NW, and characterises back-thrusts of the thrust-fault system proposed by Fiori (1991).

Near Morro Grande and Tranqueira-Pessegueiro shear zones, intense metric shear-layers with transposed primary beddings occur, where quartz-veins and millimetric venules concordant to the S_1 foliation are common (Fig. 5A).

The ductile shear is relatively prominent in the inverted flank of the recumbent folds, with important ductile deformation of the lithological sequences, and intense development of S_1, with planes associated with ruptures (Fig. 5B).

The Schmidt-Lambert diagrams (equal area) of the the S0 surface show E-W trending beds with medium dips (60º) southwards in the north flank of the Morro Grande Synform (MGS) (Fig. 6A) and N65E/80SE (and subordinately NW) in the south flank (Fig. 6B).

The S1 slaty cleavage shows preferential trending to E-W and high (80–90º) dips towards S in the north flank (Fig. 6A) and N80E/85SE-NW in the south flank (Fig. 6B), and consists of axial planes of recumbent folds (F1) subsequently disturbed by the high-angle tectonics. S1 fabrics are related with significant ductile shear, where the stretching lineations (L1) are parallel to the folds axis.

The deformation phase including the recumbent folds (F_1) is diachronic to a regional metamorphism (M_1) of variable grade, although it does not exceed the low-grade in the study area.

The transpressive tectonic event is responsible for the main structures observed in regional maps, as strike-slips

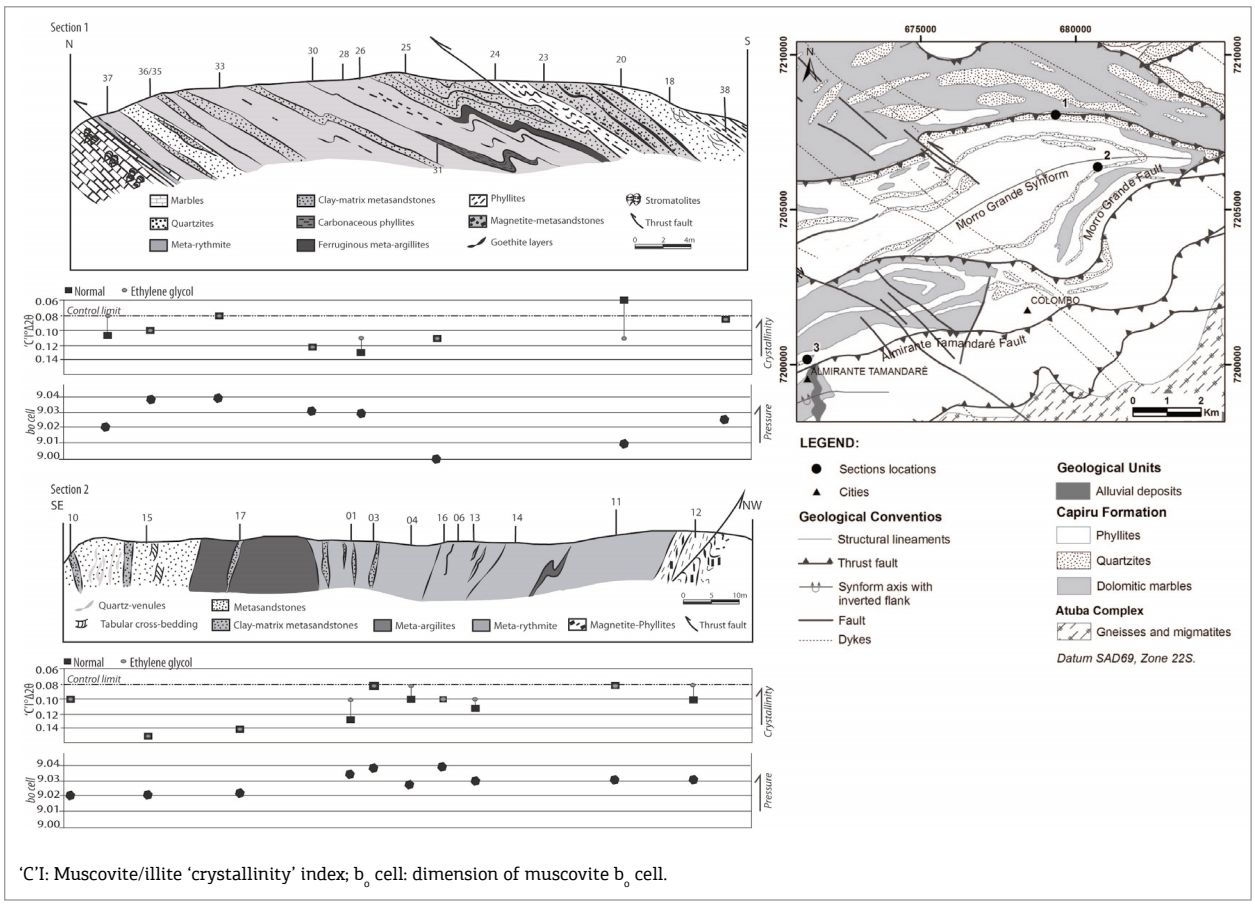

'C'I: Muscovite/illite 'crystallinity' index; b_o cell: dimension of muscovite b_o cell.

Figure 3. Crystal-chemical parameters estimated in sections 1 and 2 in the Morro Grande region. The sections locations are in the geological map. Adapted from Fiori (1985). Point 3 (in the geological map): samples used as comparative in the geobarometric study (see Table 4). Samples with differences between indexes of normal fraction and ethylene glycol treatment may present preserved expansive clay-minerals.

faults and macro-folds with preferably oriented axis to N45E and N70E (as in the Morro Grande Synform). Faleiros (2008) associates these macro-folds with *en echelon* faults and drag folds developed by a high angle tectonics strike-slip fault related.

Open-vertical folds (F_2) approximated N70E are regionally observed (Fig. 6C); they verticalize previous structures and are associated with the crenulation cleavage (S_2).

The Schmidt-Lambert diagrams of equal area of S_2 show preferential directions to N60E with high dip angles (80º) toward NW (Figs. 6A and 6B).

Associated to the genesis of this surface (S_2), the metamorphism M_2 occurs, developed under very low-grade conditions in the studied sites in the Morro Grande region.

Chemical composition

Metapelites samples from the 1:500 cross-sections were analysed by XRF and showed the following compositional variations in oxide weight total (wt%): SiO_2: 46.00–69.39, Al_3O_2: 17.81–24.94, K_2O: 0.93–10.26, MgO: 0.29–1.62; with low values of CaO (up to 0.08), Na_2O (up to 0.19), MnO (up to 0.03) and P_2O_5 (up to 0.11). A percentage of Fe_2O_3 varies from 1.89 to 13.93, and TiO_2 from 0.49 to 1.87.

The metapelites are classified as peraluminous and K-rich, with low Ca and Na, with Fe and Ti-rich types, when compared to the Post-Archean Australian Shales (PAAS) mean (Taylor & McLennan 1985) (Tab. 1).

Metasandstones have SiO_2 percentage varying from 75.56–90.76, Al_2O_3: 1.43–10.68, K_2O: 0.01–3.97, MgO: 0.00–1.04, Fe_2O_3: 0.99–13.09 with low percentage of CaO

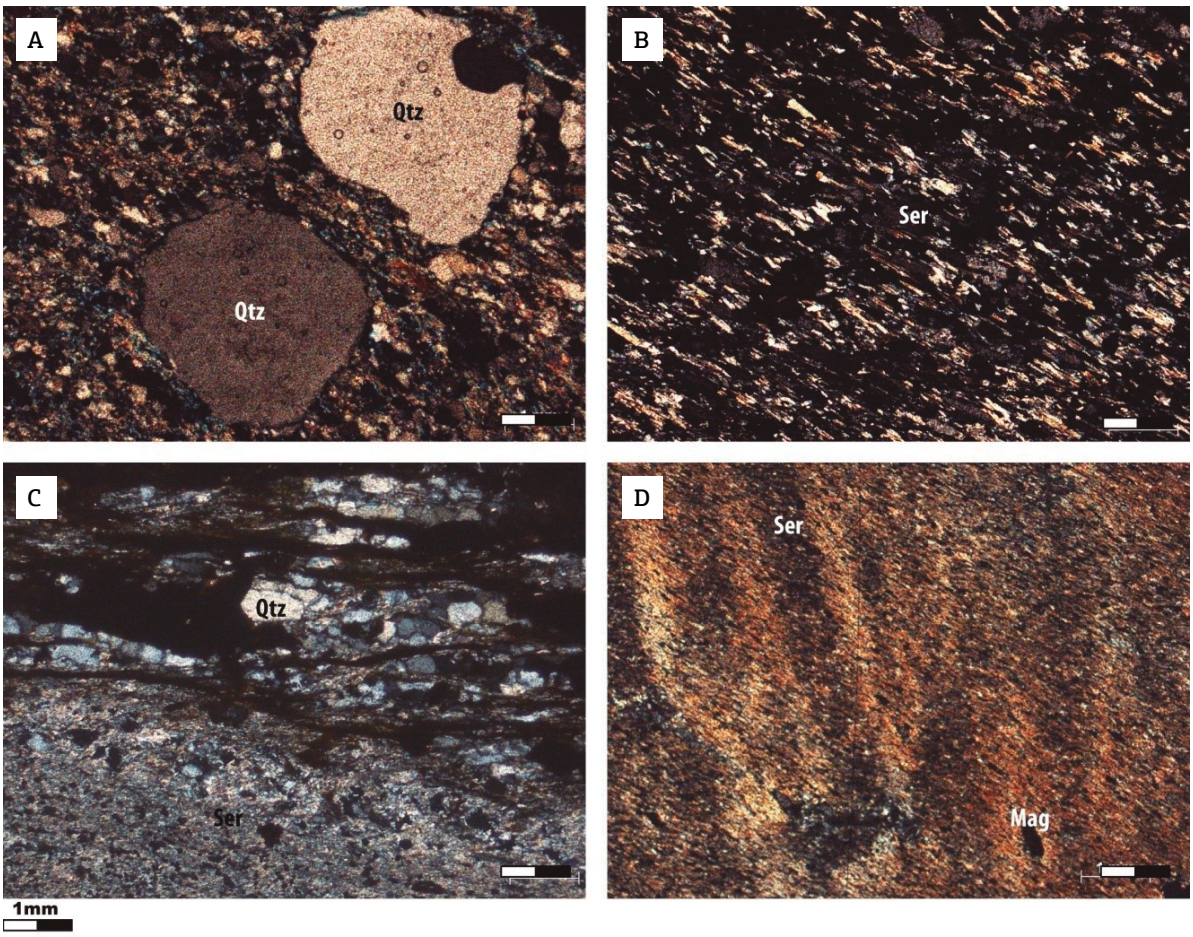

Mag: magnetite, Qtz: quartz, Ser: sericite.

Figure 4. Photomicrographs of metapelites and metasandstones from the Capiru Formation in the Morro Grande region under cross-polarized light. (A) Metasandstones with sericite matrix and quartz framework grains showing relict sedimentary structures. Sample MG-15. (B) Meta-argillite – or slate – showing well developed S_1 slaty cleavage. Sericite defines the foliation. Sample MG-11. (C) Tectonofacies of carbonaceous phyllites showing quartz intracrystalline deformation features, contacts between grains are polygonal. Sample MG-17. (D) Ferruginous phyllites with magnetite, presenting S_1 slaty cleavage, crenulated by the S_2 surface. Sample MG-12.

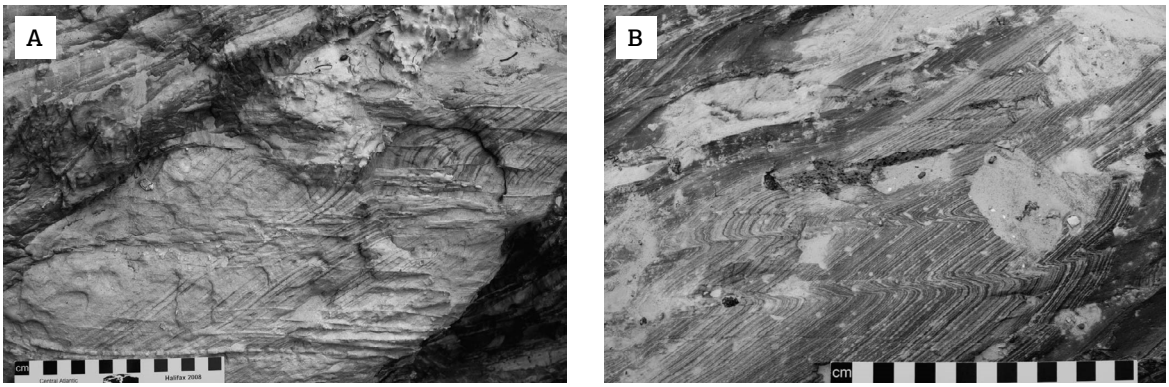

Figure 5. Structures associated to the S1 foliation development. (A) Parallel quartz micro-veins. (B) Microfolds and micro-thrusts diachronic with S1.

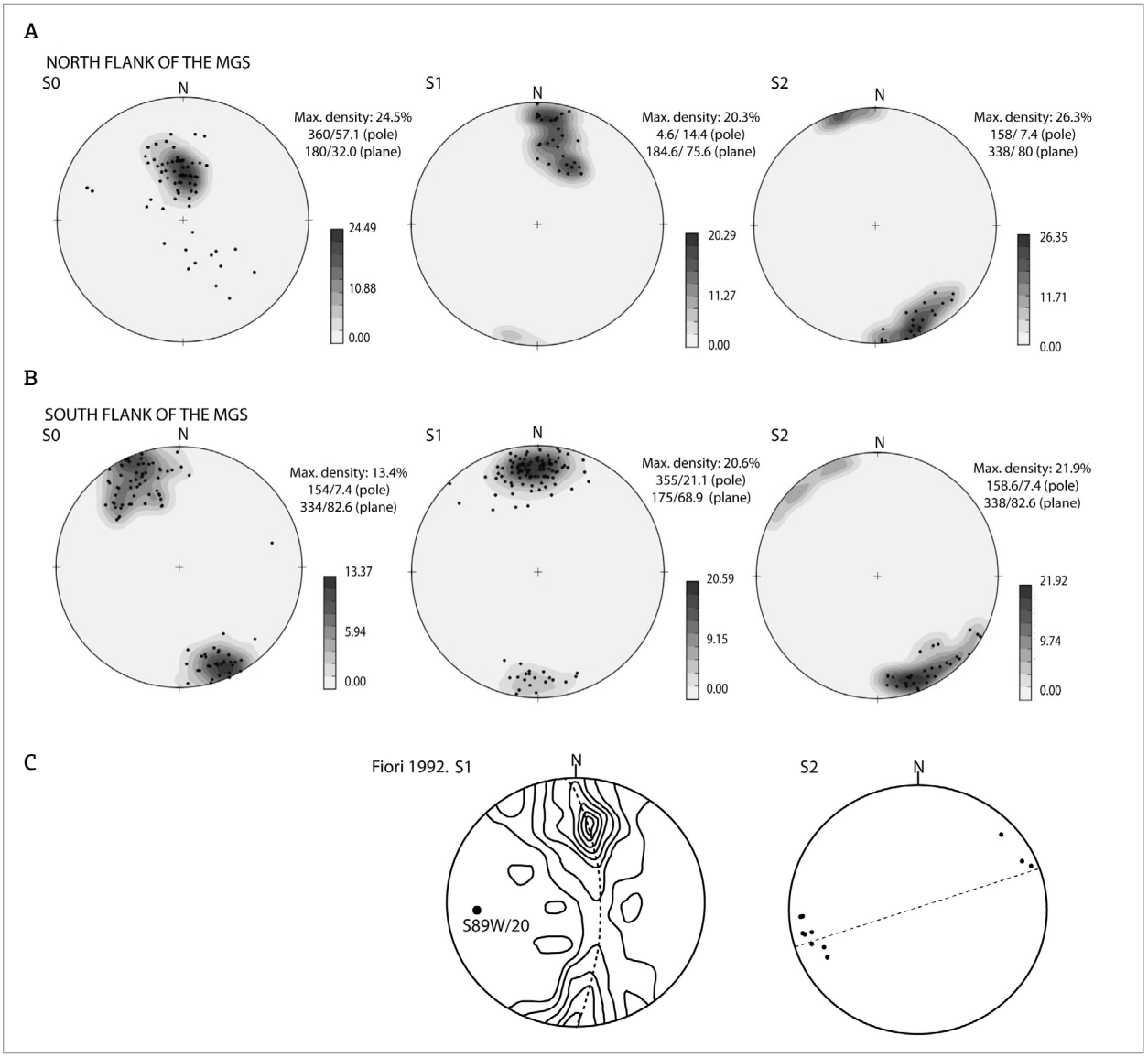

Figure 6. Sterograms of equal area, inferior hemisphere of the: (A) S_0, S_1 and S_2 surfaces in the 1 Section; (B) S_0, S_1 and S_2 surfaces in 2 Section (see Figure 3 to sections locations). (C) Stereogram of S_1 poles from Morro Grande Synform region. β axis attitude is indicated. β axis and lineation concentrations in the Setuva Antiform area (Fiori 1992).

(up to 0.04), Na_2O (up to 0.08), MnO (up to 0.03) and P_2O_5 (up to 0.04), with a clay/micaceous-matrix of different proportions (Tab. 2).

Semi-quantitative analyses presented, in some metapelites and metasandstones, iron percentages up to 13.2%, with massive goethite layers up to 80.8% of Fe_2O_3 (Tab. 3).

X-ray diffraction

The mineral assemblage of the metapelites is composed by muscovite $2M_1$ type (with phengitic composition) and it may contain quartz, kaolinite, goethite, magnetite, carbonaceous material and sepiolite, respectively, in order of abundance in the analysed samples of bulk rock and in < 2 μm fraction. There was no chlorite in the analysed samples. Mineralogy by XRD of the metapelites samples used in the crystallinity study is in Table 4.

The mineral assemblage of the metasandstones is composed by quartz, and it may contain muscovite $2M_1$ type (Grathoff *et al.* 1996), goethite and magnetite in variable proportions in the analysed samples.

Table 1. XRF bulk rock analyses of metapelites (wt% in oxide).

Sample	SiO_2	Al_2O_3	Fe_2O_3	CaO	MgO	K_2O	Na_2O	TiO_2	MnO	P_2O_5	L.O.I
MG-015-003	69.39	17.81	1.89	0.03	1.01	4.98	0.08	1.01	< 0.01	0.02	3.69
MG-015-012	59.76	22.46	4.17	0.02	1.11	6.61	0.13	1.00	< 0.01	0.04	4.47
MG-015-014	67.60	18.86	2.10	0.02	1.00	5.31	0.08	1.02	< 0.01	0.02	3.85
MG-015-016	66.22	19.58	2.20	0.02	1.08	5.62	0.09	1.01	< 0.01	0.02	3.92
MG-016-020	57.77	23.60	6.74	0.08	0.40	1.41	< 0.01	0.49	< 0.01	0.02	9.76
MG-016-024	53.43	20.84	13.93	0.02	0.29	0.93	< 0.01	1.14	< 0.01	0.06	9.44
MG-016-026	61.83	19.62	5.81	0.02	1.08	4.56	< 0.01	1.08	< 0.01	0.06	5.67
MG-016-031	46.00	31.00	3.67	0.02	1.50	10.26	0.19	1.87	< 0.01	0.04	5.08
MG-015-033	55.05	24.94	4.56	0.03	1.46	5.58	0.00	1.22	0.00	0.09	6.96
MG-016-035	59.79	20.56	4.80	0.03	1.62	7.23	0.05	1.26	0.03	0.06	4.25
MG-016-036	57.83	23.27	3.38	0.02	1.50	6.65	0.03	1.39	< 0.01	0.11	5.45
Mean	59.52	22.05	4.84	0.003	1.10	5.38	0.08	1.14	0.01	0.05	5.69
Std	5.00	2.73	2.17	0.01	0.31	1.76	0.04	0.22	0	0.02	1.66
PASS	62.80	18.00	7.22	1.30	2.20	3.70	1.20	1.00	0.11	0.16	6.00

Table 2. XRF bulk rock analyses of metasandstones (wt% in oxide).

Sample	SiO_2	Al_2O_3	Fe_2O_3	CaO	MgO	K_2O	Na_2O	TiO_2	MnO	P_2O_5	L.O.I
MG-015-006	82.24	10.68	0.99	0.02	0.51	2.71	0.04	0.42	0.00	0.01	2.36
MG-016-018	89.22	6.55	1.33	0.02	< 0.01	0.08	< 0.01	0.32	< 0.01	0.01	2.89
MG-016-023	80.64	3.66	13.09	0.02	< 0.01	0.01	< 0.01	0.08	< 0.01	0.01	2.66
MG-016-025	90.76	1.43	6.30	0.02	< 0.01	0.02	< 0.01	0.09	< 0.01	0.01	1.37
MQ-016-001	86.30	5.25	3.35	0.03	0.44	1.78	0.07	0.23	0.01	0.03	2.08
MQ-016-002	75.56	11.73	3.25	0.02	1.04	3.97	0.07	0.61	0.03	0.04	3.21
MQ-016-003	88.11	5.32	1.98	0.03	0.49	1.93	0.07	0.32	0.03	0.03	1.27
MQ-016-004	84.81	7.17	2.02	0.04	0.68	2.63	0.08	0.37	0.01	0.04	1.68
MQ-016-005	88.57	5.91	1.28	0.02	0.33	1.40	0.06	0.30	< 0.01	0.02	1.80
Mean	85.13	6.41	3.73	0.02	0.58	1.61	0.07	0.30	0.02	0.02	2.15
Std	3.84	2.33	2.65	0.01	0.19	1.10	0.01	0.12	0.01	0.01	0.56

Deformation progress and mineral phases

To select the samples used in the crystal-chemical parameters study, a SEM analysis was made to identify and to quantify the metamorphic phyllosilicate phases.

From the SEM analysis, petrographic and field data, three metamorphic facies were recognized: Ia and Ib facies, both with one metamorphic mineral phase, formed in the M_1 metamorphism; and IIa facies, with two metamorphic phases, related to the M_1 and M_2 metamorphic events.

The Ia facies show slightly oriented micas in the S_1 foliation domains, with no preferential orientation in the matrix, as shown in Figure 7A. In the transition from sedimentary and diagenetic to metamorphic illites, new grains of smectite-free illite are formed at the expense of the older minerals. This suggests that the new metamorphic minerals are recrystallized phases. Metamorphism of illites then produces new mica phases (Gharrabi *et al.* 1998). The micas of the Ia facies are considered in this study, as a new formed mica-phase.

The Ib facies show oriented micas in a pervasive S_1 slaty cleavage defined by sericite layers that form mosaics (Fig. 7B). When disturbed by the S_2 surface, the micaceous beds deform to micro-folds, but there is no mineral growth associated with the S_2 surface (Fig. 7C). With S_2 development, a new generation of metamorphic minerals is formed (IIa facies) showing growth and orientation of sericite in the S_2 crenulation cleavage (Fig. 7D).

Samples showing the two mineral phases were not considered in the crystal-chemical study.

Muscovite/illite 'crystallinity' index ('C'I)

The 'C'I were obtained through 24 metapelites samples from the Morro Grande region and are shown in Table 4. All of the 'C'I measured are smaller than 0.25 Δ2θ, suggesting an epizone or greenschist facies conditions (Kisch 1990, Warr & Rice 1994). The average 'C'I is 0.10 Δ2θ in the < 2 μm fraction, with a standard deviation of σ 0.01 Δ2θ. The 'C'I obtained in samples and its respective locations are shown in Figure 3. Sampling in the areas with well-developed S_2 crenulation cleavage (Fig. 7D) has been avoided to the 'C'I study.

Pressure conditions

As the identified paragenesis quartz ± muscovite ± goethite ± magnetite does not estimate pressure conditions because of the lack of metamorphic index minerals, the dimensions of the basal spacing (d-spacing) and the b_o cell of the K-mica were determined, to calculate the pressure conditions in the Morro Grande region studied rocks (Fig. 8).

The basal spacing in white-mica is in principle related to the paragonitic substitution in the interlayers, thus reflecting the temperature of its formation. However, the phengite content is able to modify the d-parameter (Guidotti 1984). Measurement of the K-mica b_o cell dimension, which is dependent on the degree of phengite substitution, has been related to the pressure conditions at the time of formation or recrystallization of the K-mica in the rocks (Guidotti & Sassi 1986).

The relation b_o cell increasing and decreasing basal spacing of the K-mica indicates that the d-spacing is mainly controlled by the phengite substitution and the influence of other factors is secondary (Guidotti *et al.* 1992). When this relation is satisfied, the b_o cell parameter can be used as a semi-quantitative geobarometer.

Due to the small distance along the cross-sections inside Morro Grande Synform, a few pressure differences are expected, with values increasing relatively in the proximity of the shear zones, an assumption confirmed by data (Fig. 3).

The mean value of b_o cell dimension is 9.029 A, with σ 0.008 Å, which indicates a low to intermediary pressure

Table 3. Semi-quantitative X-ray fluorescence bulk rock analyses of ferruginous metasandstones and metapelites (% in oxide).

Metapelites											
Sample	**SiO_2**	**Al_2O_3**	**Fe_2O_3**	**CaO**	**MgO**	**K_2O**	**Na_2O**	**TiO_2**	**MnO**	**P_2O_5**	**L.O.I.**
MP-016-009	63.59	17.05	9.09	0.05	0.19	2.75	0.48	1.22	0.04	0.17	4.88
Metasandstones											
Sample	**SiO_2**	**Fe_2O_3**	**Al_2O_3**	**K_2O**	**CO_2**	**MgO**	**TiO_2**	**Cl**	**P_2O_5**	**Na_2O**	**L.O.I.**
MG-016-034	69.3	13.2	9.8	2.7	<2.5	2	0.3	0.1	0.1	0	2.52
MG-016-037	65.5	7.2	17.7	3.00	4.6	0.9	0.8	0	0	0.1	0.20
Goethite layers											
Sample	**Fe_2O_3**	**SiO_2**	**MnO**	**Al_2O_3**	**MgO**	**SO_3**	**P_2O_5**	**ZnO**	**L.O.I.**		
MG-016-029	80.8	4.5	1.1	1.0	0.2	0.2	0.1	< 0.1	12.17		

gradient (Guidotti *et al.* 1992) at the time of reequilibrium of the rocks.

Considering the metamorphic grade in epizone-grade type (Frey 1987), where temperatures varies from 300–350ºC, pressures of 2– 4.5 kbar might be suggested for the M_1 metamorphism. Elevated pressure gradients (> 9.037 Å) are verified in the Almirante Tamandaré Fault region (MQ code samples) used comparatively in the geobarometric study (Tab. 4).

Table 4. Crystal-chemical parameters of metapelites of the Capiru Formation in the Morro Grande region. Used abbreviations for minerals by Kretz (1983).

Sample	Mineralogy - XRD	'C'I (Δ°2θ)		Basal spacing (Å)	b_o (Å) Ms
		B.R.	N.F. < 2 µm		
Section 1 – North flank of MGS					
MG-37	Qtz - Ms - Kln - Sep	0.13	0.08	9.941	9.022
MG-36	Qtz - Ms - Kln	0.08	0.10	9.900	9.037
MG-35	Qtz - Ms - Kln	0.07	0.10	9.915	9.039
MG-33	Qtz - Ms - Kln	0.08	0.08	9.923	9.034
MG-31	Ms – Qtz – C.M.	0.08	0.12	9.926	9.002
MG-26	Qtz - Ms - Kln	0.08	0.13	9.906	9.028
MG-20	Qtz - Ms - Kln	0.27	0.07	9.930	9.010
MG-38	Qtz – Ms	0.09	0.09	9.919	9.025
Section 2 – South flank of MGS					
MG-12	Qtz - Ms – Kln – C.M.	0.07	0.10	9.882	9.031
MG-11	Qtz – Ms- Kln	0.08	0.08	9.882	9.029
MG-13	Qtz - Ms – Kln – C.M.	0.08	0.12	9.923	9.029
MG-16	Qtz - Ms - Kln	0.08	0.10	9.938	9.034
MG-04	Qtz - Ms - Kln	0.07	0.10	9.915	9.027
MG-03	Qtz - Ms - Kln	0.07	0.08	9.865	9.039
MG-02	Qtz - Ms – Kln – C.M.	0.07	0.12	9.910	9.026
MG-01	Qtz - Ms – Kln – C.M.	0.07	0.12	9.897	9.035
MG-17	Qtz - Ms – Kln – C.M.	0.14	0.14	9.911	9.020
MG-10	Qtz - Ms - Kln	0.10	0.10	9.906	9.020
MG-15	Qtz - Ms – Kln – C.M.	0.15	0.15	9.910	9.020
Almirante Tamandaré's region fault					
MQ-01	Qtz - Ms - Kln	0.08	0.10	9.906	9.048
MQ-02	Qtz - Ms - Kln	0.08	0.12	9.925	9.041
MQ-03	Mus-Qtz	0.08	0.10	9.889	9.037
MQ-04	Mus-Qtz	0.07	0.10	9.888	9.047
MQ-05	Qtz - Ms - Kln	0.20	0.08	9.895	9.037
Mean		0.098	0.103	9.918	9.029
Standard deviation		0.033	0.016	0.017	0.008

'C'I: Ilite/muscovite crystallinity index; BR: Bulk rock; NF: Normal fraction. The samples' location can be visualized on Figure 13. MG samples: (Sections 1 and 2); MQ samples: Morro do Quartzito, Almirante Tamandaré fault region, used for parameters comparison; Qtz: quartz; Ms: muscovite; Kln: kaolinite; Sep: sepiolite; C.M.: carbonaceous material.

4.1 Bulk organic carbon content (BOC)

The meta-argillites and carbonaceous phyllites samples were analysed for their BOC. In four samples, the BOC content ranged from 0.09 up to 1.21 (%), characterizing preserved organic matter (OM) in the metapelites of the Capiru Formation.

These results were balanced with the respective nitrogen amount that ranged from 0.02 up to 0.50 (%), which displays good correlation with the carbon content, typical of OM, denoting low thermal maturity and subsequent low crystallinity degree of the organic matter.

Conditions for the preservation of low-crystallinity OM accumulated in orogens may be consulted in Dalla Torre *et al.* (1996) and Potel *et al.* (2006).

The accumulated organic matter in the metapelites of the Morro Grande region occurs dispersed, related to the lithotypes which have larger amount of clay-minerals, suggesting

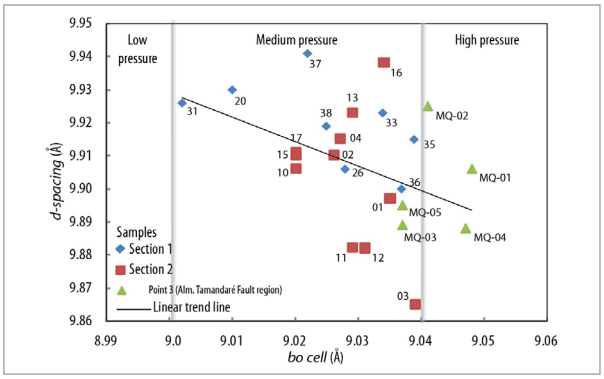

Figure 8. Cross-plot showing the basal spacing (d-spacing) versus b_0 dimensions of K-mica. The more pressure, the d-spacing of K-mica reduces. The regression line of total data represents this main trend. The relation indicates that the d-spacing is controlled by phengitic substitution, and the other factors are secondary (paragonite substitution, for instance). Adapted by Guidotti et al. (1992).

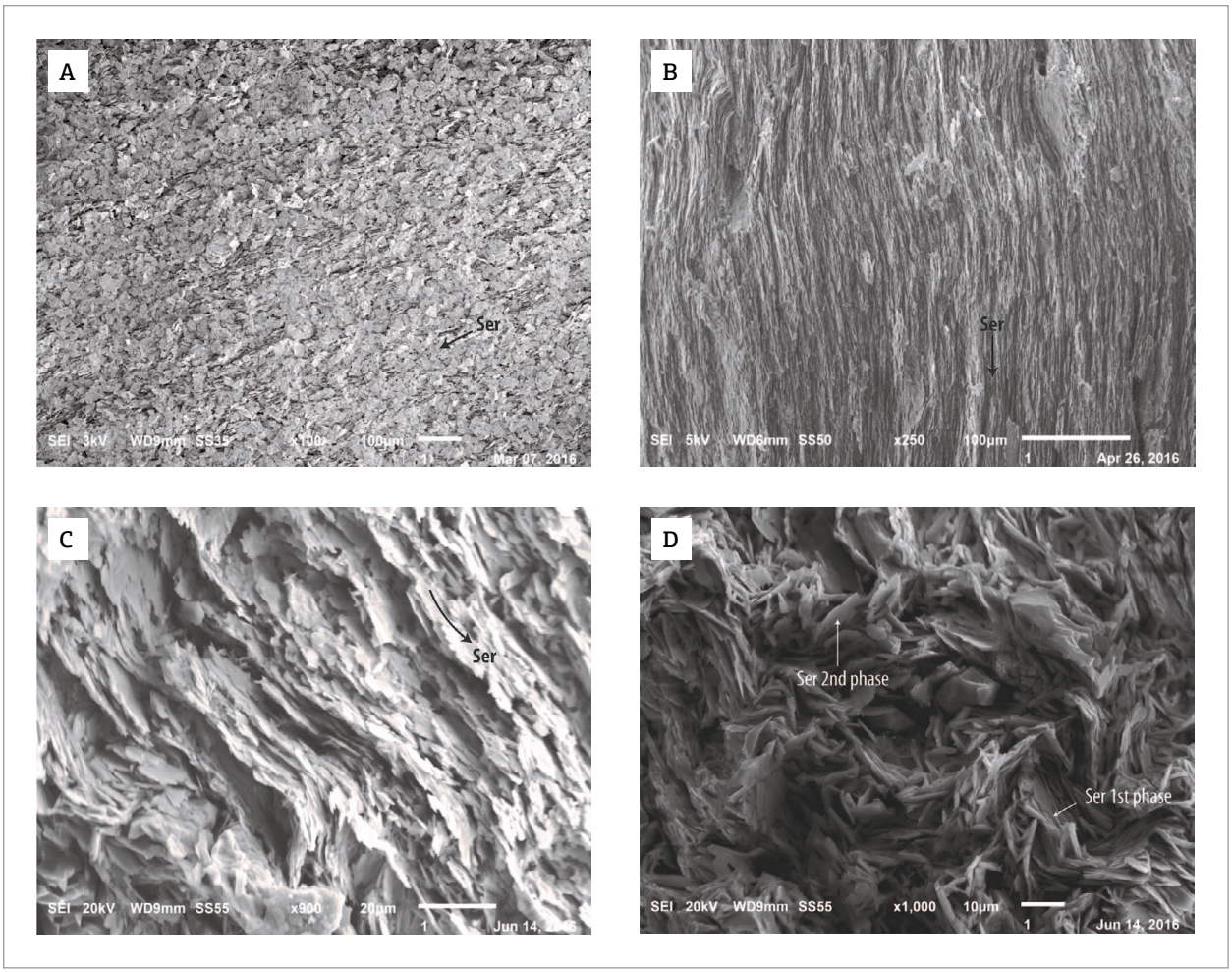

Figure 7. Scanning Electron Microscopy (SEM) Photomicrographs of the metapelites from Capiru Formation. (A) Ia facies in metapelites – or slates - from the souh flank of the Morro Grande Sinform (MGS). Sericite is slightly oriented in S_1 surfaces (micas from the metamorphic phase) in the non-oriented matrix (relict phase) - Sample 15. (B) Layered sericite in the Ib facies. Flank North of the MGS. Sample 31. (C) Crenulated S_1 surfaces, without mineral growth in S_2 foliation. Ib facies. Sample 32. (D) IIa facies showing mineral growth in S_2 surfaces in carbonaceous phyllites. Hinge of the Morro Grande Synform. Samples with two phases of serecite have not been used in this study for crystallinity index.

an accumulation process by trapping-by clay-minerals originally expansive, as smectite.

DISCUSSION

The Capiru Formation in the Morro Grande region displays a lithologic variability relative to the granulation of the lithotypes, with similar mineralogical compositions. The main mineral paragenesis is quartz ± muscovite ± iron oxides, at different assemblages, containing mainly kaolinite as associated mineral. Iron oxides include magnetite and goethite, characterizing meta-stable phases depending on the metamorphic conditions. Goethite occur as layers parallel to the S_0 bedding and remobilized next to major shear zones, while magnetite occurs disseminated in slightly deformed zones.

The presence of relict minerals and grains, and portions with preserved framework is common, where the textures and structures of the protolith are evident. These zones contrast with the NE-trending tectonofacies that generate phyllites and quartzites with penetrative metamorphic foliation presence.

The relationship between measured parameters is shown in Figure 3. Comparisons between 'C'I and b_o cell may be done, since the 'C'I in the Morro Grande region is lower than 0.25º 2θ, validating the using of b_o cell parameter, as suggested by Guidotti and Sassi (1986).

The metapelites 'C'I values indicate that the studied rocks metamorphic grade is consistent with the greenschist facies ($\Delta 2\theta < 0.25$) (Frey 1991). They also demonstrate a good correlation with b_o cell values, where discrepant results are related to the presence of carbonaceous material (Fig. 3).

The macro- and microscopic deformation ranges are also recognized when crystal-chemical parameters are evaluated: the samples position within the cross-sections and its relation with the tectonic structures demonstrates 'C'I strongly controlled by strain effects, with variation up to 0.035º $\Delta 2\theta$ in the lithotypes close to the mapped shear zones (Fig. 3). The number of samples and the presence of thrust faults along the profiles prelude the use of curve fitting procedures to compare de 'C'I values with strain. Therefore, although the relation between both is qualitatively clear, as demonstrated by Gutiérrez-Alonso & Nieto (1996), we cannot propound an equation of general use.

Studies with 'C'I increasing values respectively with strain, fluid circulation, development of tectonic microstructures and metamorphic foliation may be consulted in Frey *et al.* (1980), Merrimann *et al.* (1995), Gutiérrez-Alonso & Nieto (1996), Poyatos *et al.* (2001) and Potel *et al.* (2006).

Nevertheless, the 'C'I diminish in samples with the presence of organic matter. An explanation to this fact could be the temperature isolating effect promoted by the carbonaceous material in the organic rich rocks.

The expected temperatures for the epizone/greenschist facies obtained through the 'C'I would be about 300–350ºC, but, due to the strain influence on these rocks, such temperature cannot represent reality, making the 'C'I rather overestimated, and by consequence, the estimated metamorphism temperatures.

The increase in the metamorphic grade, with the deformation progress is well established, but the mechanisms by which deformation can enhance the metamorphic grade are not fully understood, thus a kinect interpretation seems to offer a better explanation for certain features of mineralogical development at low temperatures than the effects of the temperature itself in a dynamic metamorphic context (Poyatos *et al.* 2001).

The covariance between the 'C'I and the b_o cell dimension (Fig. 3) supports the hypothesis that these indicators are controlled by a strain/pressure relationship.

The calculated K-mica b_o cell dimensions show good correlation with identified shear zones *versus* preserved zones. The b_o cell dimensions suggest the highest pressure peak that the rocks were submitted to, and indicate that the metamorphism M_1 acted in a more efficient way in the metapelites studied in Morro Grande, due to the results of the b_o cell and its relation with structures of D_1 being extremely close.

The samples with the highest b_o cell dimensions are located near the Almirante Tamandaré Fault (Fig. 3) used in this study as a comparative site, to evaluate the b_o cell dimensions under relative high-pressure conditions (greenschist facies – up to garnet zone), according to the classification proposed by Guidotti and Sassi (1986).

One of the most notable features about deformation in the Morro Grande Synform is about the heterogeneities in S_1 foliation development. The studied distribution of crystal-chemical parameters allows for the interpretation related to D_1 deformation and the concomitant generation of S_1 surface in the studied cross-sections:

- The S_1 slaty cleavage can be related to recumbent folding generation, where the ductile shear is prominent in the inverted flanks of the folds, that shows intense foliation development;
- The shear and recumbent folding are interpreted as conjugated structures developed at the hanging wall of the main thrust faults, trending to SE quadrant, in a fold-and-belt-thrust system, with main trending movement from NW towards SE, where the Capiru Formation stands as a allochtonous unit regarding the subjacent unit, represented by the Atuba Complex.

All the organic-rich samples demonstrated preserved organic matter, even at low quantities. The organic matter content indicates that the coalification degree in Morro Grande Synform range from very low to low.

It is important to emphasize that, through petrography/geochemical studies, graphite or semi-graphite contents were not observed. This result is discrepant when compared to the obtained 'C'I, normally comparable indexes. Most correlations between those indicators are found at sites where the geodynamic conditions of predominant Barrovian orogenic metamorphism. Furthermore, organic matter is usually more sensitive to tectonic shear/strain than clay-minerals (Dalla Torre *et al.* 1997, Suchy *et al.* 1997, Sakaguchi *et al.* 2007). However, an organic matter maturation delay is observed in Morro Grande Synform. Explanation for this phenomenon is addressed by Dalla Torre et al. (1996a); studying lithotypes from the Diablo Range, where discrepant values of organic matter maturation and 'C'I were also observed. Potel *et al.* (2006) compared exhumation paths at New Caledonia and found an increase in OM maturation values along high pressure — low temperature (HP-LT) sectors, concluding then, that contrasts on PT paths are also responsible for the differences on the maturation indexes in terrains with similar metamorphic conditions.

In Diablo Range the exhumation occurs through a cold trajectory, allowing the maximum maturity reached by the organic matter to be maintained. In contrast, in the New Caledonia, the pressure — temperature (PT) retrogressive path is adiabatic, with temperature increase, which explains the high crystallinities reached by the organic matter. Thus, explanations for the delay in OM maturation in Capiru Formation may be related to the metamorphic grade and differences of temperature in the different sectors, the PT paths and the exhumation trajectories, still poorly understood.

Metamorphic conditions

Based on the studied crystal-chemical parameters, the metamorphism of the Capiru Formation in the Morro Grande Region is typical of epizone (Frey 1991) or greenschist facies (Winkler 1974). With the b_o cell estimated data, registered temperatures of 300–350ºC with estimated pressures between 2.5 and 4.5 kbar, indicate a low to intermediate pressure gradient within the low-grade context.

Although records of a posterior tectonics that affected Morro Grande Synform rocks were found through petrography, in this study, the metamorphism (M_2) does not produce recrystallization, mineral reaction or retrograde metamorphism in the studied samples, being the calculated metamorphic conditions exclusively from the M_1 phase.

However, temperatures obtained through crystal-chemical parameters may be overestimated due to the rock deformation. Despite a series of variables involved in the OM maturation, the presence of preserved OM in the metapelites may indicate temperature gradients, thus avoiding its coalification. Furthermore, the absence of chlorite inside preserved sectors as a metamorphic index mineral might be interpreted due to thermal insufficiency during metamorphism, although protolith features such as the lack of trioctaedric clay-minerals assemblage decline the possibility of chlorite-growth.

Taking into account the presented criteria, the temperature required for the M_1 metamorphism in the studied rocks is considered then, between 250 (minimum temperature) and 350ºC, with pressures between 2.5 and 4.5 kbar, which may represent a subgreenschist (Frey 1991) evolving to a greenschist type-metamorphism (Fig. 9).

Tectono-thermal setting of the Capiru Formation

The petrological data of Morro Grande succession allow for an interpretation of metamorphic conditions developed under low temperatures (250–350ºC), supported by the illite cristallinity index, low-maturation of the organic matter and mineral relicts, at tectonic slices inner sectors.

At the slice-edges chlorite-growth is rarely observed (Figs. 10A and 10B), though it occurs as an intermediate-member, most of the time, totally consumed to the biotite formation (Fig. 10C).

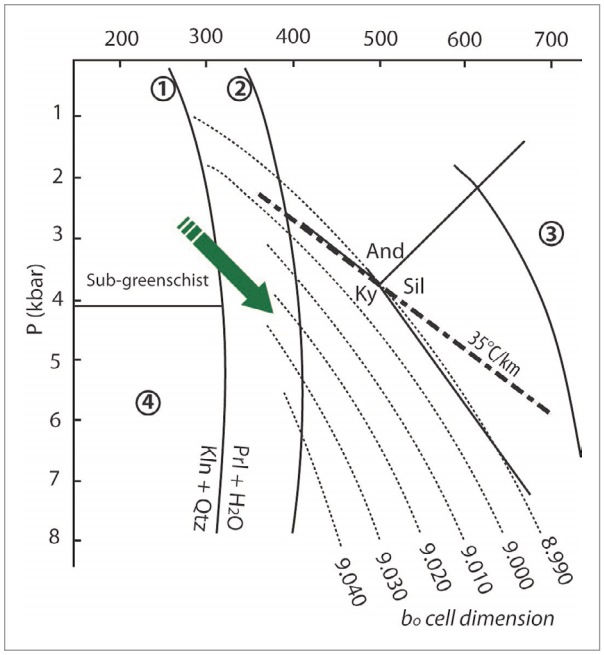

Figure 9. P-T diagram demonstrating the variation of b_o cell values (dotted lines). The arrow indicates the range of estimated pressure values and temperature of the M_1 metamorphism in the studied areas. Relationship between the Al-silicates phases are shown (Holdaway 1971); other reaction curves represented: 1) kaolinite + quartz = pyrophyllite + H_2O; 2) pyrophyllite = Al-silicates + quartz + H_2O; 3) staurolite + quartz + muscovite = Al-silicate + biotite + H_2O (Greenwood 1976); 4) maximum glaucophane stability (Maresch 1977). Modified from Guidotti and Sassi (1986). A geothermic gradient of 35ºC/km is used as reference (traced line).

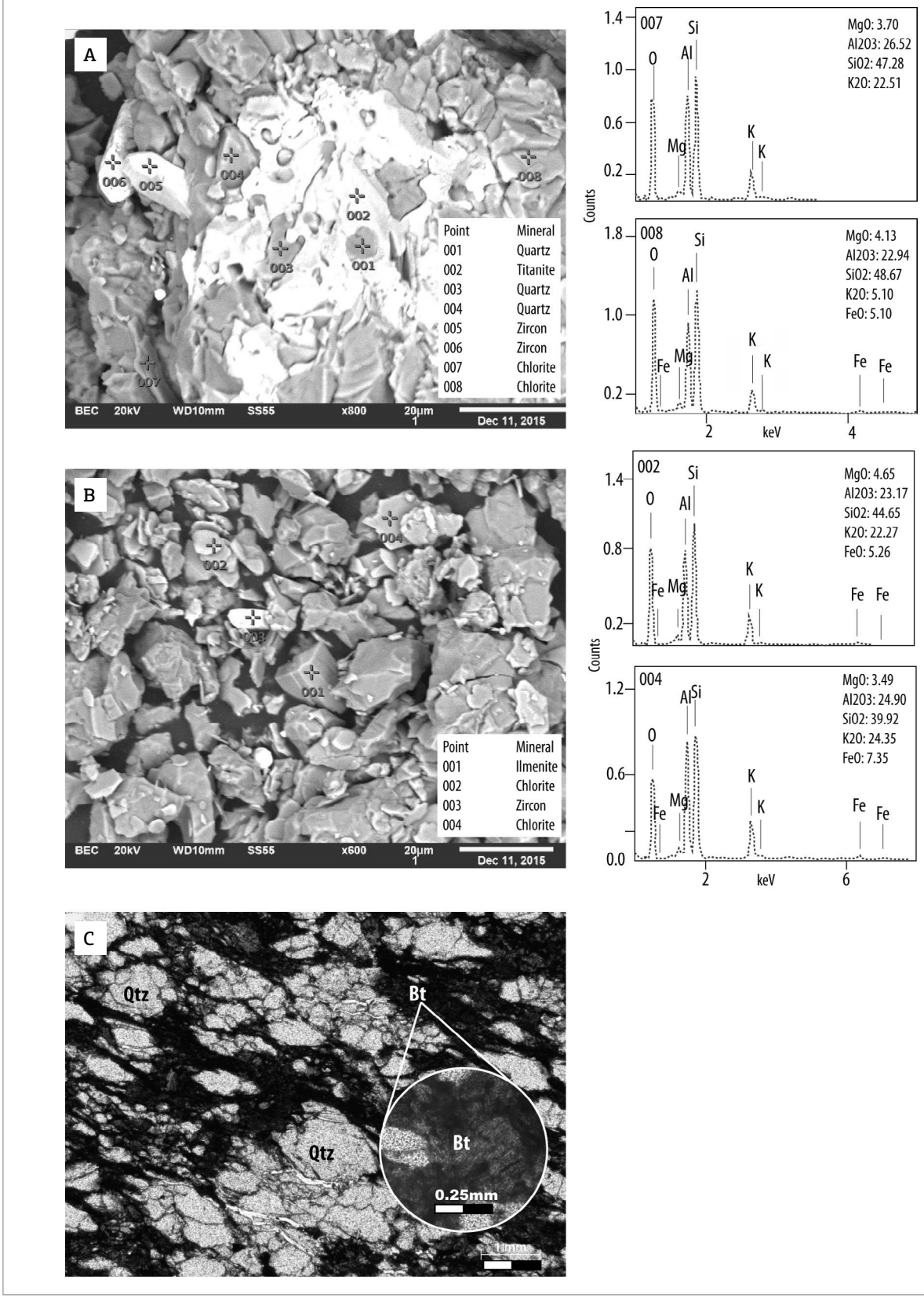

Figure 10. (A) SEM-EDS photomicrography of metasandstone showing quartz framework and sericite/chlorite (point 7 and 8) aggregates. Morro Grande Synform hinge. (B) SEM-EDS photomicrography of meta-argilite with quartz framework and chlorite (point 2 and 4) matrix. Morro Grande Synform axis. Zircon, titanite and ilmenite are the main acessory minerals. (C) Biotite-quartz-magnetite metasandstone, Tranqueira-Pessegueiro Fault area.

The tectonic pattern of Capiru Formation can be defined such as an intensely deformed sequence, with strong tectonic control, but within a stratigraphic context still well-preserved, consistent with a thrust-and-fold-belt formed in a superior crustal level, related to a progressive-type metamorphism.

The records of M_1 metamorphism (S_1, D_1 folds and thrusts) were deformed in the late stages of the orogen, during the transpressive phase, which modified the original set of S_0 and S_1, without a significant metamorphism in the Morro Grande Synform region. However, the metamorphic peak in Capiru Formation is related to a metamorphic phase widely observed northward, responsible for the distribution of the main paragenesis observed in Capiru Formation (Fig. 11). The chlorite contents increases from south, where its occurrence is subordinate, northward, where the main recognized structure is a low-angle Sm_2 crenulation cleavage (Faleiros 2017)/ mylonitc foliation (Patias 2016), transposing the S_1 slaty cleavage. To Faleiros (2017), the occurrence of biotite and kyanite-growth is sin-kinematic to Sm_2 and the paragenesis denote minimum temperatures of 380–430ºC and pressures above 2.5 kbar at sites with higher PT conditions.

The metamorphic range of Capiru Formation varies from low-grade conditions with incomplete paragenesis (as in the Morro Grande Synform region), with minimum temperatures of 250ºC, reaching metamorphic conditions of greenschist facies – up to biotite zone (up to 420ºC) and rare occurrence of above-Barrovian paragenesis with kyanite-biotite bearing types, as described by Faleiros (2017) and staurolite-biotite, kyanite-biotite and silimanite-kyanite denoting higher PT conditions, as observed by Patias (2016).

The Capiru Formation exhibits a typical geometry of low-grade metamorphic belt due to the major differences that usually occur in metamorphic thermobaric conditions, structural style and deformation mechanisms (Frey 1991). The south portion show a thin-skinned deformation style, lack of Sm_2 cleavage development, evolving to a syn-metamorphic deformation where the Sm_2 cleavage is a widespread pervasive structure (Faleiros 2017, Patias 2016), accompanied by highly strained rocks leading to fabrics of progressive penetrativeness northwards. The Morro Grande Synform region displays a tectonic and metamorphic frame consistent with the cold sectors of the low-grade belt within an orogen context.

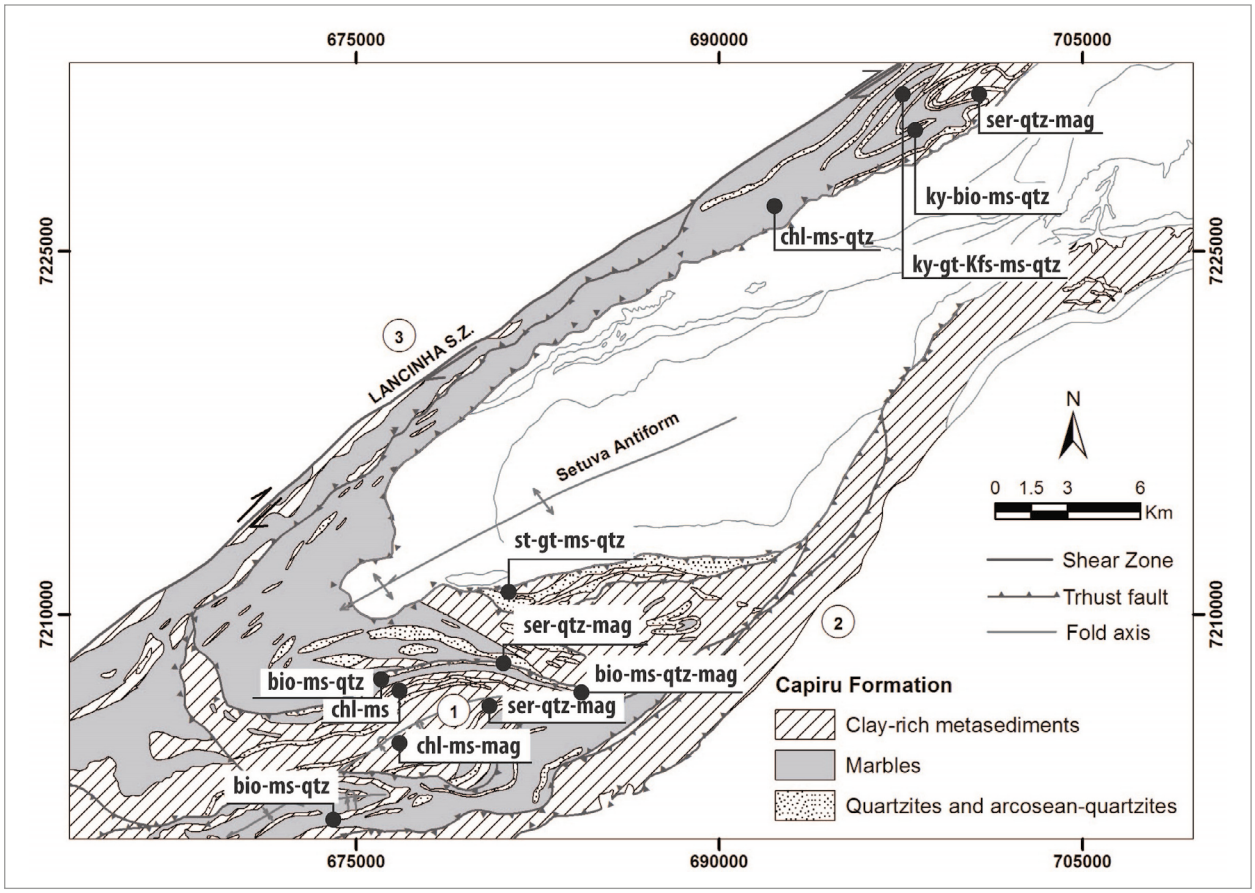

Figure 11. Main paragenesis distribution of the Morro Grande Synform (1). This work, Fiori (1991), Leandro (2016), Santos (2017). North sector of the Capiru Formation (Patias 2016); (2) Atuba Complex; (3) Apiaí Terrane.

CONCLUSIONS

According to the phase sequence occurred in the Morro Grande Synform region, the relationship between deformation and low metamorphic grade are summarized in the following conclusions:

- The thrust tectonic in the Morro Grande region was delevoped under low-temperature conditions (epizone), with low organic matter maturation and preservation of mineral relicts;
- During shear and diachronic recumbent folding, the ductile shear was developed specially in the surroundings of the major shear zones and in the inverted flanks of the recumbent folds, generating fabrics and high-strain zones verified in field work as tectonofacies;
- In terms of metamorphism, the 'C'I showed differences in the deformed zones, indicating different temperature gradients in several sectors of the Morro Grande Synform, while relevant paragenesis with index minerals development are rarely observed. The studied metamorphic gradients show different temperatures, where reactions close to the equilibrium conditions occur only at restrict portions;
- Metamorphic fluids and supplemented energy through the strain, might have helped, through reaction progress, the growth of new minerals and the complete illite transformation in its polytypes, until it reaches muscovite M_1 typical crystallinities; and
- The metamorphic grade and the estimated pressure are superior in M_1 metamorphism in the studied rocks, indicating that the acting of the M_2 phase on the study area was incipient.

ACKNOWLEDGEMENT

The authors acknowledge the financial support provided by CNPq (Conselho Nacional de Desenvolvimento Científico e Tecnológico), and are thankful for the support with the "*Projeto Capiru*" (CNPq 481429/2013) and the GEOBIOCAL Project (FJPL – UFPR - FUNPAR), and research grants. They would also like to thank Dr. Almério Barros França, Dr. Silvana Bressan Riffel and Dr. Carlos Eduardo de Mesquita Barros for the suggestions and comments made for the improvement of this paper.

REFERENCES

Ackermann L., Langer K., Rieder M. 1993. Germanium muscovites with excess hydroxil water, $KAl_2[Ge_{3-x}Al_{1+x}O_{10-x}(OH)^*(OH)_2]$ and the question of the excess OH in natural muscovites. *European Journal of Mineralogy*, **5**:19-30. DOI: 10.1127/ejm/5/1/0019

Bahniuk A.M. 2007. *Controles geológicos da carstificação em metadolomitos da Formação Capiru – Neoproterozoico, região metropolitana de Curitiba/PR*. Dissertation, Universidade Federal do Paraná, Curitiba, 138 p.

Bigarella J.J., Salamuni R. 1956. Estudos preliminares da Série Açungui. v. estruturas organógenas nos dolomitos da Formação Capiru (estado do Paraná). *Dusenia*, **7**(6):317-23.

Dalla Torre M, de Capitani C., Frey M., Underwood M.B., Mullis J., Cox C. 1996. Very-low temperature metamorphism of shales from Diablo Range, Franciscan Complex, California: new constrains on the exumation path. *Geological Society of America Bulletin*, **108**:578-601. https://doi.org/10.1130/0016-7606(1996)108<0578:VLTMOS>2.3.CO;2

Dalla Torre M., Ferreiro Mählmann R., Ernst W.G. 1997. Experimental study on the pressure dependence of vitrinite maturation. *Geochimica et Cosmochimica Acta*, **61**:2921-2928. https://doi.org/10.1016/S0016-7037(97)00104-X

Faleiros F.M. 2008. *Evolução de terrenos tectono-metamórficos da Serrania do Ribeira e Planalto Alto Turvo (SP, PR)*. PhD Thesis, Instituto de Geociências, Universidade de São Paulo, São Paulo, 306 p.

Faleiros F.M. 2017. Metamorfismo e termobarometria de pelitos da Formação Capiru: Implicações tectônicas para a Faixa Ribeira Meridional. *In*: X International Symposium on Tectonics, Salvador, *Short Papers*, p. 109-111.

Faleiros F.M., Campanha G.A., Martins L., Vlach S.R.F., Vasconcelos P.M. 2011. Ediacaran high-pressure collision metamorphism and tectonics of the Southern Ribeira Belt (SE Brasil): Evidence for terrane accretion and dispersion during the Gondwana assembly. *Precambrian Research*, **189**:263-291. https://doi.org/10.1016/j.precamres.2011.07.013

Fiori A.P. 1985. *Mapa geológico e estrutural da região de Rio Branco – Bocaiúva do Sul*. SG – 22-X-D. Minerais do Paraná S.A. Curitiba – PR, mapa geológico, escala 1:100.000. Curitiba.

Fiori A.P. 1991. *Tectônica e Estratigrafia do Grupo Açungui a norte de Curitiba, São Paulo*. PhD Thesis, Instituto de Geociências, Universidade de São Paulo, São Paulo, 261 p.

Fiori A.P. 1992. Tectônica e estratigrafia do Grupo Açungui, PR. *Boletim de Geociências – USP. Série Científica*, **23**:55-74.

Fiori A.P. 1994. Evolução geológica da Bacia Açungui. *Boletim Paranaense de Geociências*, **42**:7-27.

Fiori A.P., Gaspar L.A. 1993. Considerações sobre a estratigrafia do Grupo Açungui (Proterozóico Superior), Paraná, Sul do Brasil. *Série Científica*, **24**:1-19. http://dx.doi.org/10.11606/issn.2316-8986.v24i0p1-19

Frey M. 1987. *Low temperature metamorphism*. New York, Chapman & Hall, 351 p.

Frey M. 1991. *Low-grade metamorphism*. London, Wiley, 328 p.

Frey M., Teichmüller M., Teichmüller R., Mullis J., Künzi B., Breitschmid A., Grüner U., Schwizer B. 1980. Very low-grade metamorphism in external parts of the Central Alps: illite crystallinity, coal rank and fluid inclusion data. *Eclogae Geologicae Helvetiae*, **73**:173-203.

Gharrabi M., Velde B., Sagon J.P. 1998. The transformation of illite to muscovite in pelitic rocks: constraints from X-ray diffraction. *Clays and clay Minerals*, **46**:79-88. DOI: 10.1346/CCMN.1998.0460109

Grathoff G.H., Moore D.M. 1996. Illite polytype quantification using Wildfire calculated X-ray diffraction patterns. *Clays and Clay Minerals*, **44**(6):835-842. DOI: 10.1346/CCMN.1996.0440615

Greenwood H.J. 1976. Metamorphism at moderate temperatures and pressures. *In*: D. K. Bailey D.K., Macdonald R. (eds.), *The Evolution of the Crystalline Rocks*. New York, Academic Press, p. 187-259.

Guidotti C.V. 1984. Micas in metamorphic rocks. *In*: Bailey S.W. (ed.), *Reviews in mineralogy and Geochemistry*. Mineral Society of America, v. 13, p. 357-467.

Guidotti C.V., Mazzoli C., Sassi F.P., Blencoe J.G. 1992. Compositional controls on the cell dimensions of $2M_1$ muscovite and paragonite. *European Journal of Mineralogy*, **4**(2):283-298. DOI: 10.1127/ejm/4/2/0283

Guidotti C.V., Sassi F.P. 1986. Classification and correlation of metamorphic facies series by means of muscovite b_o data from low-grade metapelites. *Neues Jahrbuch fur Mineralogie, Abhandlungen*, **153**:363-380.

Gutiérrez-Alonso G, Nieto F. 1996. White-mica "cristallinity", finite strain and cleavage development across a large Variscan structure, NW Spain. *Journal of the Geological Society*, **153**:287-299. https://doi.org/10.1144/gsjgs.153.2.0287

Holdaway M.J. 1971. Stability of andalusite and the aluminosilicate phase diagram. *American Journal of Science*, **271**:97-131. DOI: 10.2475/ajs.271.2.97

Juschaks L. 2006. *Fácies, estruturas biogênicas e modelos deposicionais dos Metadolomitos da Formação Capiru – Grupo Açungui, Neoproterozoico do Paraná*. Dissertation, Programa de pós-graduação em Geologia, Universidade Federal do Paraná, Curitiba, 100p.

Juster T.C., Brown P.E., Bailey S.W. 1987. NH_{4-} bearing illite in very low grade metamorphic rocks associated with coal, northeastern Pennsylvania. *American Mineralogist*, **72**:555-565. DOI: 0003-004x/8 7/0506-05

Kisch J. 1990. Calibration of the anchizone a critical comparison of illite 'cristallinity' scales used for definition. *Journal of Metamorphic Geology*, **8**:31-46. DOI: 10.1111/j.1525-1314.1990.tb00455.x

Kretz R. 1983. Symbols of rock-forming minerals. *American Mineralogist*, **68**:277-279. DOI: 0003-.fix)vE3/0r02-0277$02.ffi

Kübler B. 1968. Evaluation quantitative du métamorphisme par la cristallinité d l'illite. *Bulletin du Centre de Recherches de Pau*, **2**:385-397.

Leandro R. 2016. *Caracterização tectonoestratigráfica das sequências terrígenas do Conjunto Morro Grande, Formação Capiru – PR*. Dissertation, Programa de Pós-graduação em Geologia, Universidade Federal do Paraná, Curitiba, 121 p.

Leandro R., Santos L.R., Cury L.F. 2017. A sequência terrígena Capiru: Registro de ambiente estuarino do Esteniano (1.08 – 1.20 Ga.) na região de Morro Grande – Norte de Curitiba/PR. (no prelo).

Maresch W.V. 1977. Experimental studies on glaucophane: an analysis of present knowledge. *Tectonophysics*, **43**:109-125. https://doi.org/10.1016/0040-1951(77)90008-7

Merriman R.J., Peacor D.R. 1999. Very low-grade metapelites: mineralogy, microfabrics and measuring reaction progress. *In*: Frey M., Robinson D., *Low-grade Metamorphism*. Oxford, Blackwell Sciences, p. 10-60.

Merriman R.J., Roberts B., Peacor D.R., Hirons, S.R. 1995. Strain-related differences in the crystal growth of white mica and chlorite: a TEM and XRD study of the development of metapelitic microfabrics in the Southern Uplands thrust terrane, Scotland. *Journal of Metamorphic Geology*, **13**:559-576. DOI: 10.1111/j.1525-1314.1995.tb00243.x

Patias D. 2016. *Caracterização tectono-metamórfica dos paragnaisses da região do Campestre, Cerro Azul – PR*. Graduation Project, Universidade Federal do Paraná, Curitiba, 70 p.

Potel S., Ferreiro Mählmann R., Stern W., Mullis J., Frey M. 2006. Very Low-grade Metamorphic Evolution of Pelitic Rocks under High-pressure/Low-temperature Conditions, NW New Caledonia (SW Pacific). *Journal of Petrology*, **47**(5):991-1015. https://doi.org/10.1093/petrology/egl001

Poyatos D.M., Nieto F., Azor A., Simancas J.F. 2001. Relationships between very low-grade metamorphism and tectonic deformation: examples from the southern Central Iberian Zone (Iberian Massif, Variscan belt). *Journal of the Geological Society*, **158**:953-968. https://doi.org/10.1144/0016-764900-206

Robert J.L., Beny J.M., Della Ventura G., Hardy M. 1993. Fluorine in micas: crystal-chemical control of the OH-F distribution between trioctahedral and dioctahedral sites. *European Journal of Mineralogy*, **5**:7-18. DOI: 10.1127/ejm/5/1/0007

Roberts B., Merriman R.J. 1985. The distinction between Caledonian burial and regional metamorphism in metapelites from north Wales: An analysis of isocryst patterns. *Journal of the Geological Society*, **142**:615-624. https://doi.org/10.1144/gsjgs.142.4.0615

Robinson D., Merriman R.J. 1999. Low-temperature metamorphism: an overview. *In*: Frey M, Robinson D. *Low-grade metamorphism*. Oxford, Blackwell Science, p. 1-9.

Robinson D., Warr L.N., Bevins R.E. 1990. The illite 'crystallinity technique': a critical appraisal of its precision. *Journal of Metamorphic Petrology*, **8**:333-344. DOI: 10.1111/j.1525-1314.1990.tb00476.x

Santos L.R. 2017. *Metamorfismo de baixo grau nas rochas metassedimentares terrígenas da Formação Capiru na região do Morro Grande, Colombo-PR*. Dissertation, Programa de Pós-graduação em Geologia, Universidade Federal do Paraná, Curitiba, 121 p.

Sakaguchi A., Yanagihara A., Ujiie K., Tanaka I., Kameyama M. 2007. Thermal maturity of a fold–thrust belt based on vitrinite reflectance analysis in the Western Foothills complex, western Taiwan. *Tectonophysics*, **443**:220-232. DOI: 10.1016/j.tecto.2007.01.017

Sassi F.P., Scolari A. 1974. The b_o value of potassium white micas as a barometric indicator in low-grade metamorphism of pelitic schists. *Contributions to Mineralogy and Petrology*, **45**:143-152.

Siga Jr. O. 1995. *Os domínios tectônicos do sudeste do Paraná e nordeste de Santa Catarina: geocronologia e evolução crustal*. PhD Thesis, Instituto de Geociências, Universidade de São Paulo, São Paulo, 212 p.

Silva I.E. 2010. *Estromatólitos registrados no Conjunto Litológico Rio Branco (Formação Capiru, Grupo Açungui)*. Dissertation, Programa de Pós-graduação em Geologia, Universidade Federal do Paraná, Curitiba, 112 p.

Suchy V., Frey M., Wolf M. 1997. Vitrinite reflectance and shear-induced graphitization in orogenic belts: A case study from the Kandersteg area, Helvetic Alps, Switzerland. *International Journal of Coal Geology*, **34**:1-20. https://doi.org/10.1016/S0166-5162(97)00018-9

Summons R.E., Hallmann C. 2014. Organic geochemical signatures of early life on Earth. *In*: Turekian K.K., Holland H.D. (eds.), *Treatise on Geochemistry*, 2ª ed. Amsterdam, Elsevier, v. 12, p. 33-46.

Taylor S.R., McLennan S.H. 1985. *The Continental Crust:* Its Composition and Evolution. Oxford, Blackwell, 312 p.

Warr L.N., Rice A.H. 1994. Interlaboratory standardization and calibration of clay mineral crystallinity and crystallite size data. *Journal of Metamorphic Geology*, **12**:141-152. DOI: 10.1111/j.1525-1314.1994.tb00010.x

Watanabe K., Naraoka H., Wronkiewicz D.J, Condie K.C., Ohmoto H. 1997. Carbon, nitrogen, and sulphur geochemistry of Archean and Proterozoic shales from the Kaapvaal Craton, South Africa. *Geochimica et Cosmochimica Acta*, **61**:3441-3459. https://doi.org/10.1016/S0016-7037(97)00164-6

Winkler H.G.F. 1974. *Petrogenesis of metamorphic rocks*, 3ª ed. Berlin, Springer, 320 p.

© 2018 Sociedade Brasileira de Geologia
This is an open access article distributed under the terms of the Creative Commons license.